Electronic Supplementary Material (ESI) for CrystEngComm.

Tin-Assisted Growth of All-Inorganic Perovskite Nanoplatelets with Controllable Morphologies and Complementary Emissions

Yanxi Ding[a], Tan Li[a], Xiaoyun Li[a], Emmanuel Acheampong Tsiwah[a], Chengzhen Liu[a], Peng Gao[b,*], Tao Zeng[c], Yunxia Chen[c,d], Xiujian Zhao[a], Yi Xie[a,*]

[a] *State Key Laboratory of Silicate Materials for Architectures, Wuhan University of Technology (WUT), No. 122, Luoshi Road, Wuhan 430070, P. R. China.*

[b] *Laboratory of Advanced Functional Materials, Xiamen Institute of Rare-earth Materials, Chinese Academy of Science, No 1300 Jimei Road, Jimei District, 361021, Xiamen, Fujian, P.R. China.*

[c] *School of Materials Science and Engineering, Jingdezhen Ceramic Institute (Xianghu Campus), Xianghu Road, Jingdezhen, Jiangxi 333403, P.R. China.*

[d] *National Engineering Research Center for Domestic & Building Ceramics, Jingdezhen Ceramic Institute (Xinchang Campus), Taoyang Southern Road, Jingdezhen, Jiangxi, 333000, PR China.*

Email:xiey@whut.edu.cn; peng.gao@fjirsm.ac.cn.

Contents

1. Characterization of the $CsPbBr_3$ nanocrystals achieved in the presence of $SnBr_4$

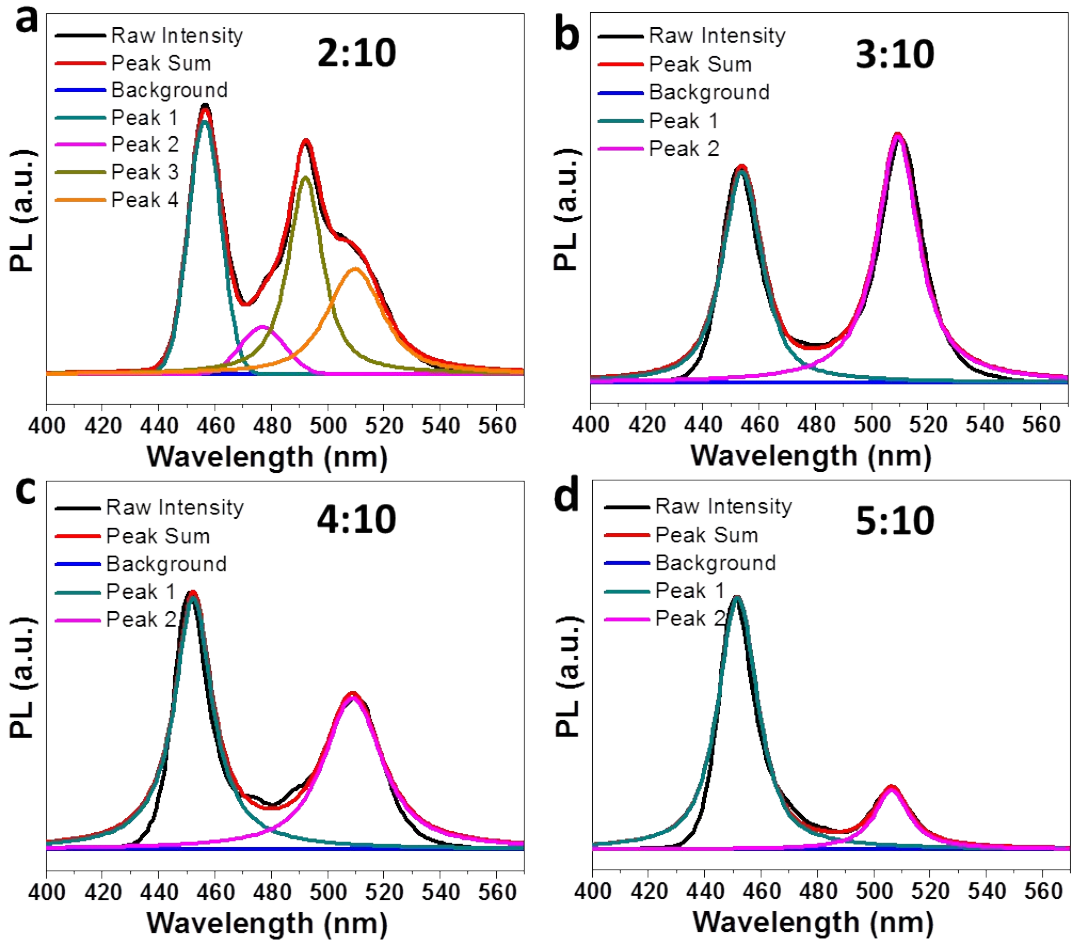

Fig. S1. *Multi-peak fitting of the PL spectra for the $CsPbBr_3$ nanocrystals achieved with different Sn:Pb precursor ratios as dictated. The multi-peak-emitting spectra were fitted by the type of Gaussian. The peak positions extracted from the fit are listed in Table S1. The results indicate that the as-synthesized samples consist of NPLs with different sizes (in thickness). The samples are synthesized in the presence of $SnBr_4$.*

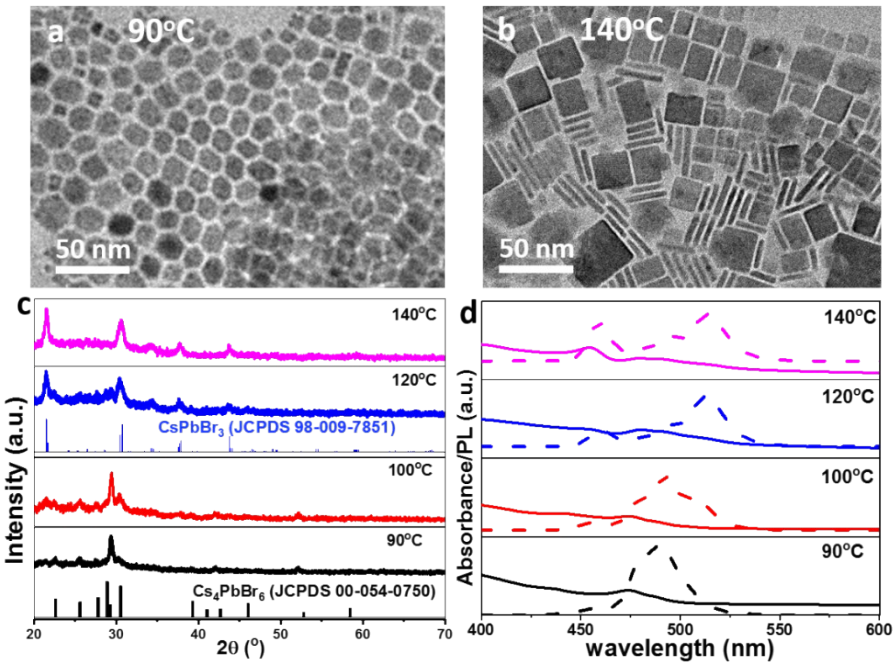

Fig. S2. *TEM images (a-c), optical absorbance spectra (d) and PL (e) of the aliquots of the $CsPbBr_3$ nanocrystals achieved at different temperatures as dictated, in the absence of precursor Sn:Pb ratios of 2:10. The samples are synthesized in the presence of $SnBr_4$.*

Table S1. *The summarization on the optical characterization of the $CsPbBr_3$ nanocrystals achieved in the presence of different Sn:Pb precursor ratios.*

Sn:Pb ratio	PL peaks[a] (nm)				FWHM[b] (nm)			
	Peak1	Peak 2	Peak 3	Peak 4	Peak1	Peak 2	Peak 3	Peak 4
2:10	456.4	477.0	492.0	509.8	13.7	18.8	14.5	23.5
3:10	454.1	509.3			16.8	17.7		
4:10	452.4	509.0			16.2	24.9		
5:10	451.8	506.5			16.9	14.9		

[a] Dual PL peaks after deconvolution.

[b] Full width at half-maximum (FWHM) of each PL peak after deconvolution.

2. Characterization of the $CsPbCl_xBr_{3-x}$ nanocrystals achieved in the presence of $SnCl_4$

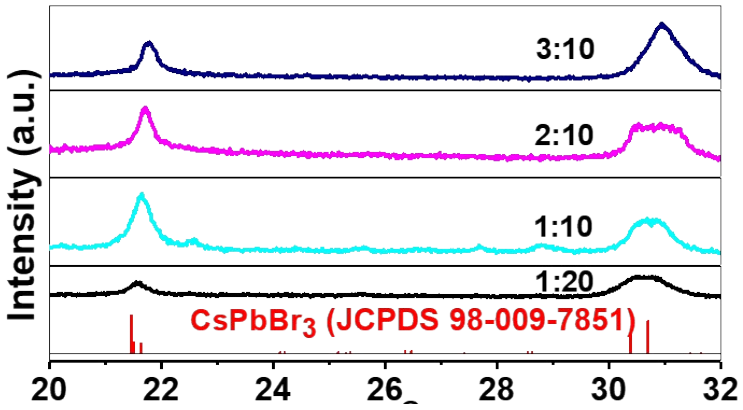

Fig. S3. *XRD patterns raging 20-32 degree of the $CsPbCl_{3-x}Br_3$ nanocrystals achieved with different precursor Sn:Pb ratios as dictated. All the nanocrystals are obtained in the presence of $SnCl_4$.*

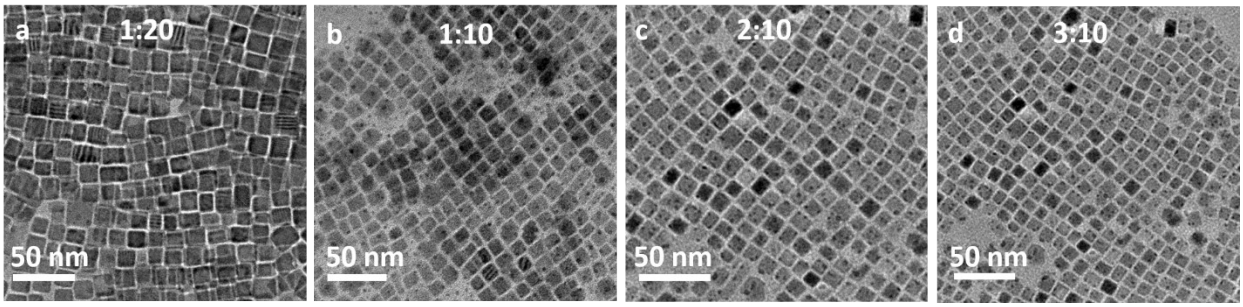

Fig. S4. *TEM images of the perovskite $CsPbCl_{3-x}Br_3$ NC achieved with different precursor Sn:Pb ratios as dictated. All the nanocrystals are obtained in the presence of $SnCl_4$.*

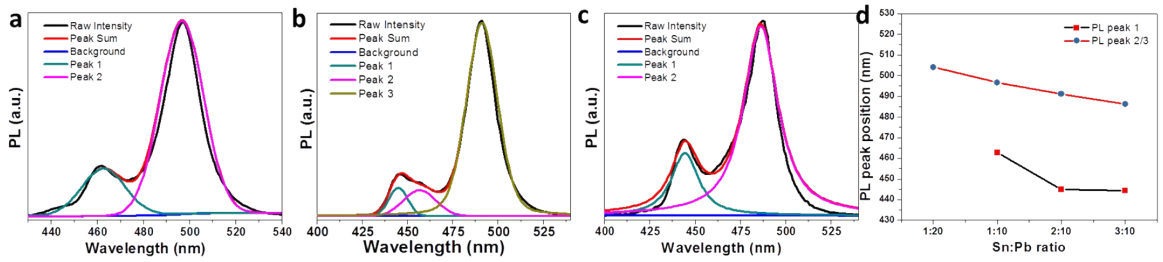

Fig. S5. *(a-c) Deconvolution of the PL spectra collected on the $CsPbCl_{3-x}Br_3$ nanocrystals achieved with precursor Sn:Pb ratios of 1:10 (a), 2:10 (b) and 3:10 (c). For data fitting, a doublet was used for each PL spectrum. All the nanocrystals are obtained in the presence of*

$SnCl_4$. (d) PL peak wavelength positions of the fitted peaks of the various $CsPbCl_{3-x}Br_3$ nanocrystals achieved with different precursor Sn:Pb ratios.

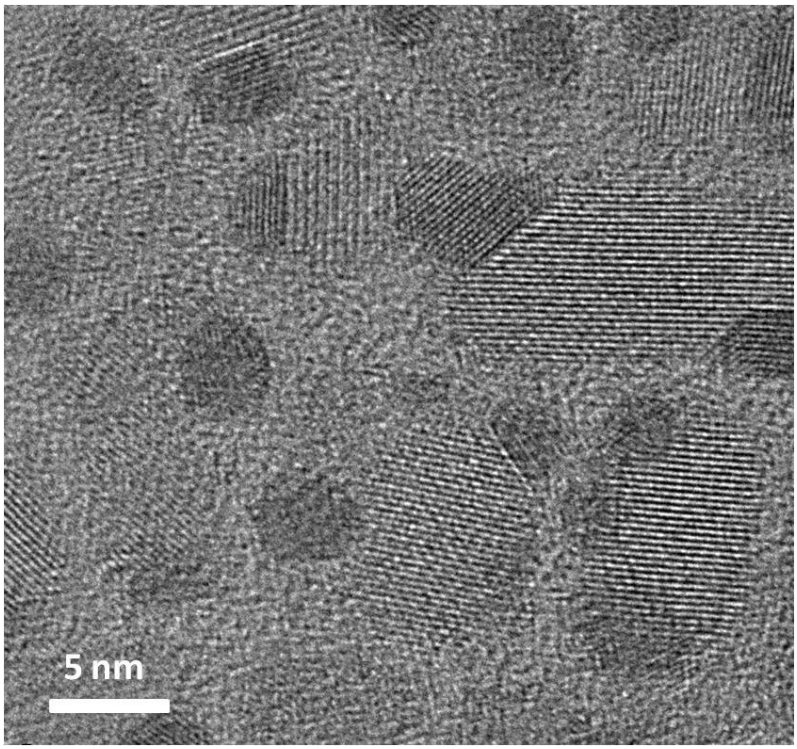

Fig. S6. *HRTEM image of $CsPbCl_{3-x}Br_3$ nanocrystals upon E-beam irradiation for 10 seconds. The sample was prepared in the presence of $SnCl_4$, by fixing precursor Sn:Pb molar ratio as 2:10.*

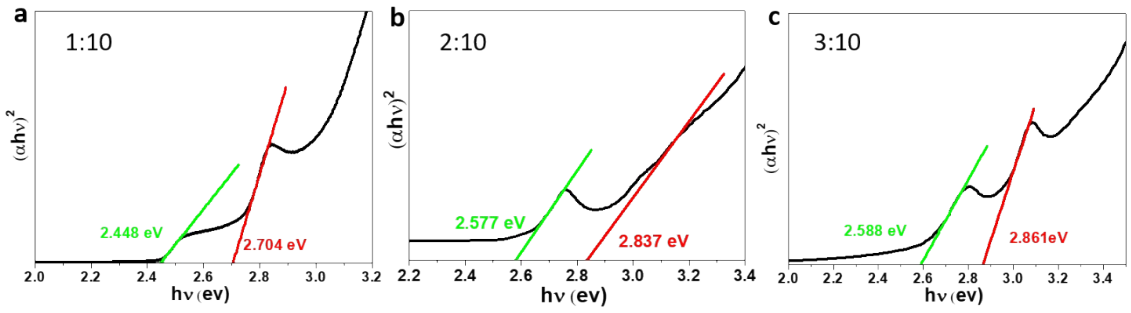

Fig. S7. *Tauc plots of $CsPbBr_3$ nanocrystals formed in the presence of different precursor Sn:Pb ratios as dictated. The samples are synthesized in the presence of $SnCl_4$.*

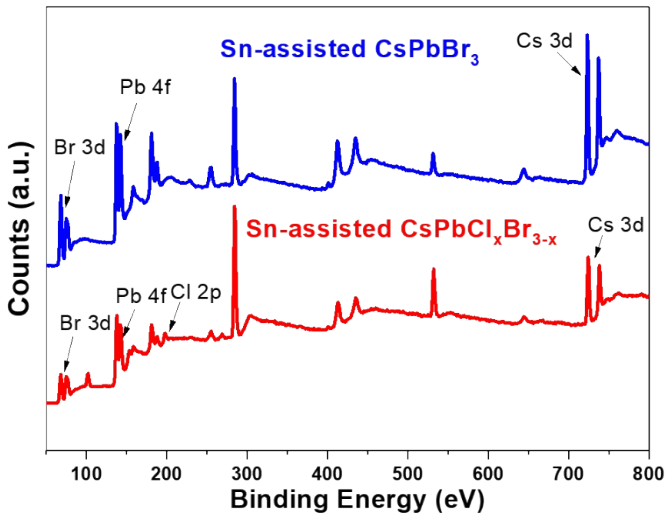

Fig. S8. *Survey XPS of Sn-directed synthesized $CsPbBr_3$ nanocrystals and $CsPbCl_xBr_{3-x}$ in the presence of $SnBr_4$ and $SnCl_4$, respectively. It is noteworthy that no Sn signal can be detected in all the as-synthesized samples. Cl signals is present in the sample collected when $SnCl_4$ is added.*

3. Characterization of the $CsPbBr_3$ nanocrystals achieved in the presence of $SnBr_2$ under Ar atmosphere

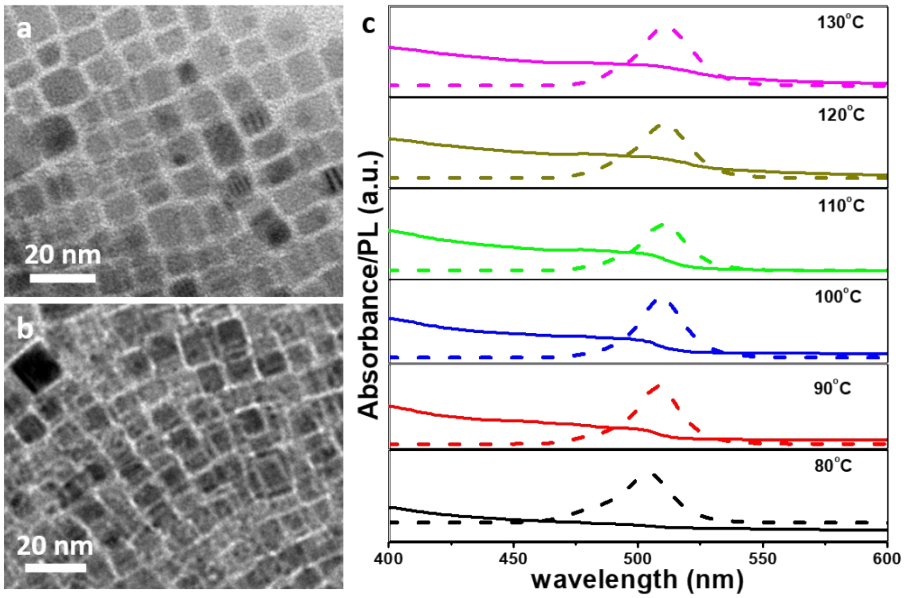

Fig. S9. *(a-b) TEM images of the $CsPbBr_3$ nanocrystals achieved at 100°C (a) and 130°C (b), respectively. (c) Optical absorbance spectra (solid lines) and PL (dash lines) of the aliquots of the $CsPbBr_3$ nanocrystals achieved at different temperatures as dictated, in the presence of precursor $SnBr_2$ under Ar atmosphere.*

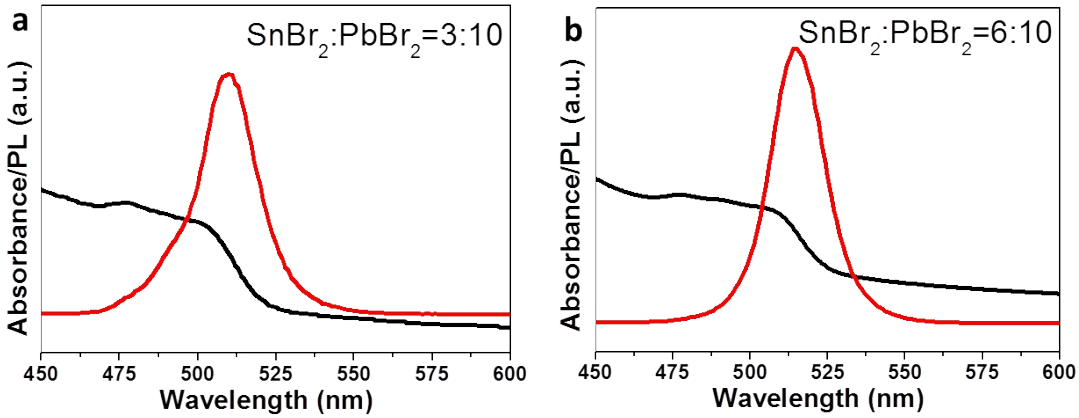

Fig. S10. *Optical absorbance spectra (black lines) and PL (red lines) of $CsPbBr_3$ nanocrystals achieved in the presence of different amounts of $SnBr_2$ (denoted as Sn:Pb as dictated) under Ar atmosphere.*

4. Characterization of the perovskite $CsPbCl_{3-x}Br_3$ NC synthesized in the presence of $SnCl_2$ under Ar atmosphere

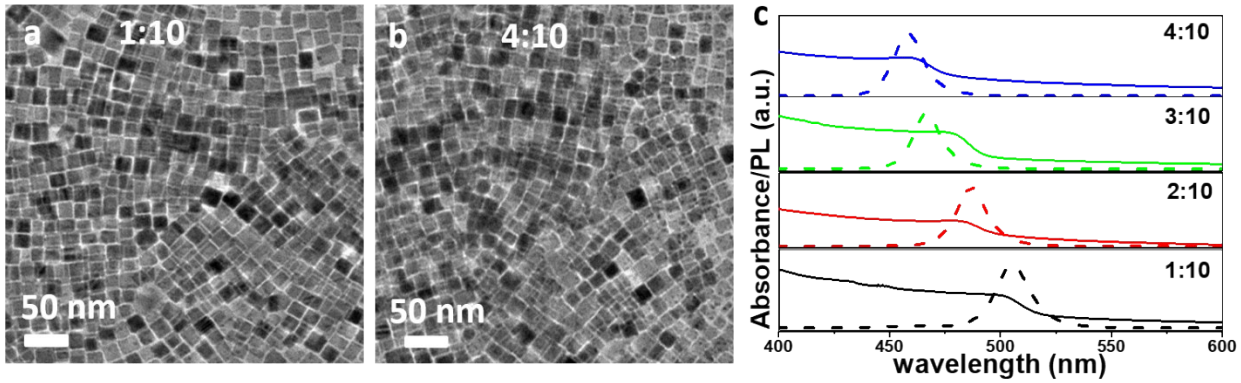

Fig. S11. *(a-b) TEM images and (c) absorption spectra (solid curves) and PL emissions (dash curves) of the $CsPbCl_xBr_{3-x}$ nanocrystals synthesized in the presence of $SnCl_2$ under Ar atmosphere, with different precursor Sn:Pb ratios as dictated.*

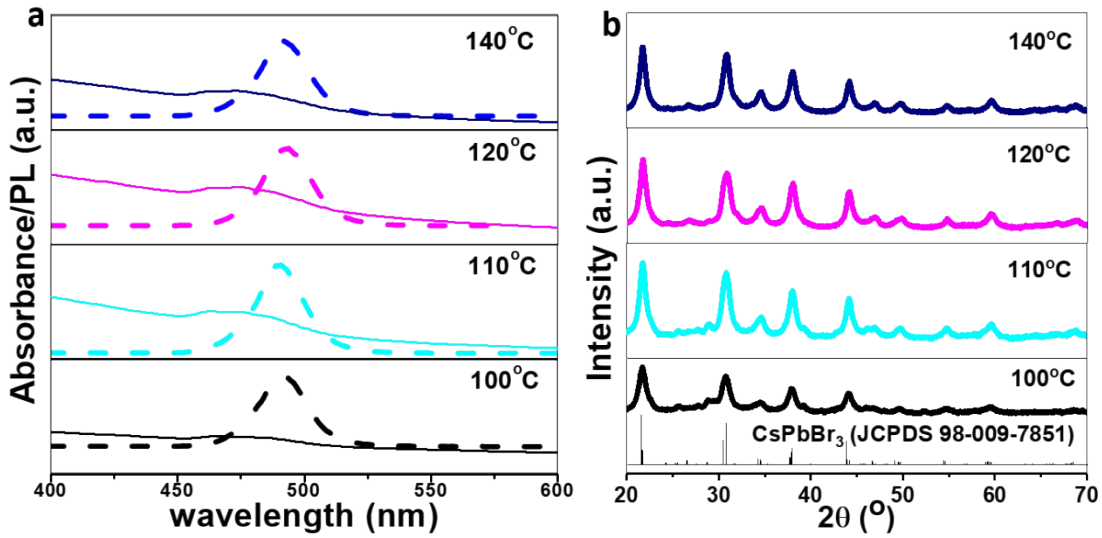

Fig. S12. *Optical absorbance spectra and PL (a) and XRD patterns (b) of the aliquots of the $CsPbBr_3$ nanocrystals achieved at different temperatures as dictated, in the absence of precursor Sn:Pb ratio of 2:10.*

5. Characterization of the $CsPbBr_3$ nanocrystals achieved in the presence of $SnBr_2$ in the open air

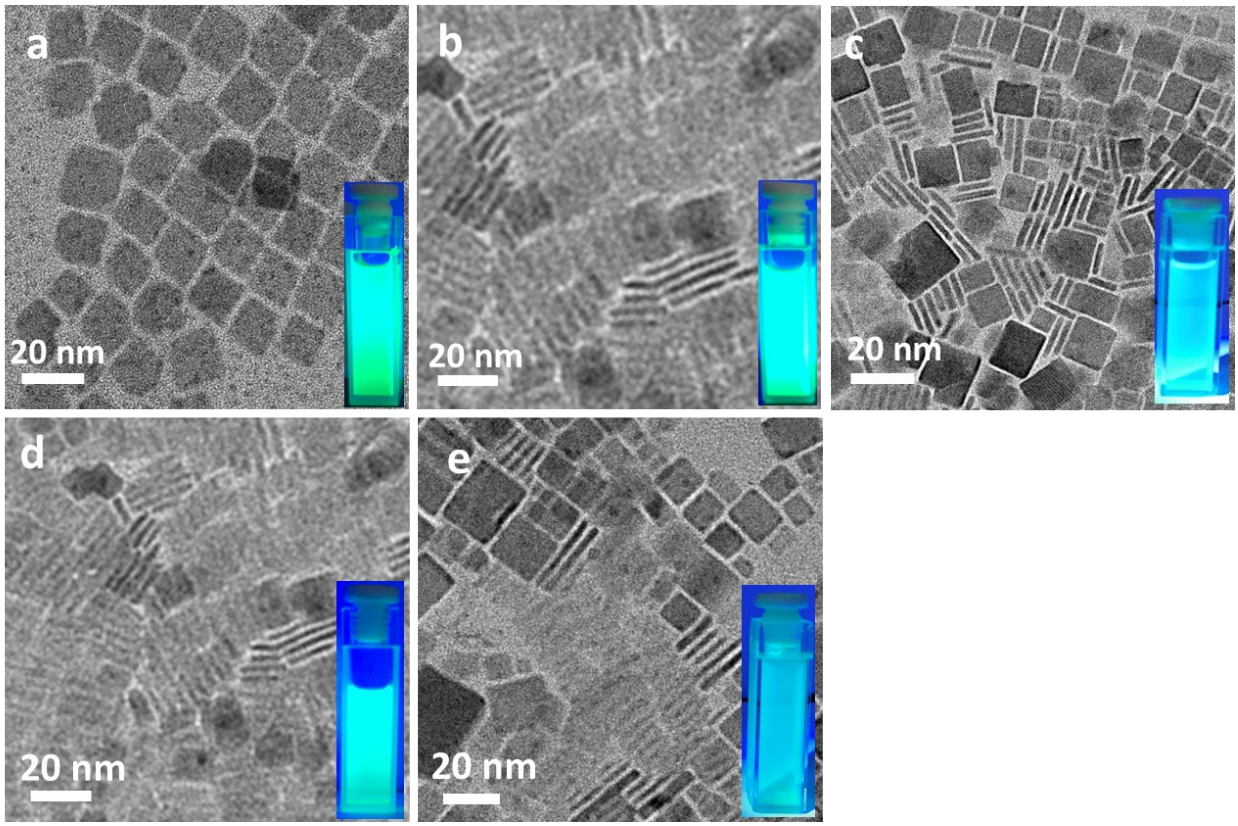

Fig. S13. *TEM images of the perovskite $CsPbBr_3$ NC achieved with precursor Sn:Pb ratios of 1:10 (a), 2:10 (b), 3:10 (c), 4:10 (d) and 5:10 (e). Insets in each panel present the photographs of corresponding nanocrystals dispersed in hexane under UV light illumination (355 nm excitation wavelength).*

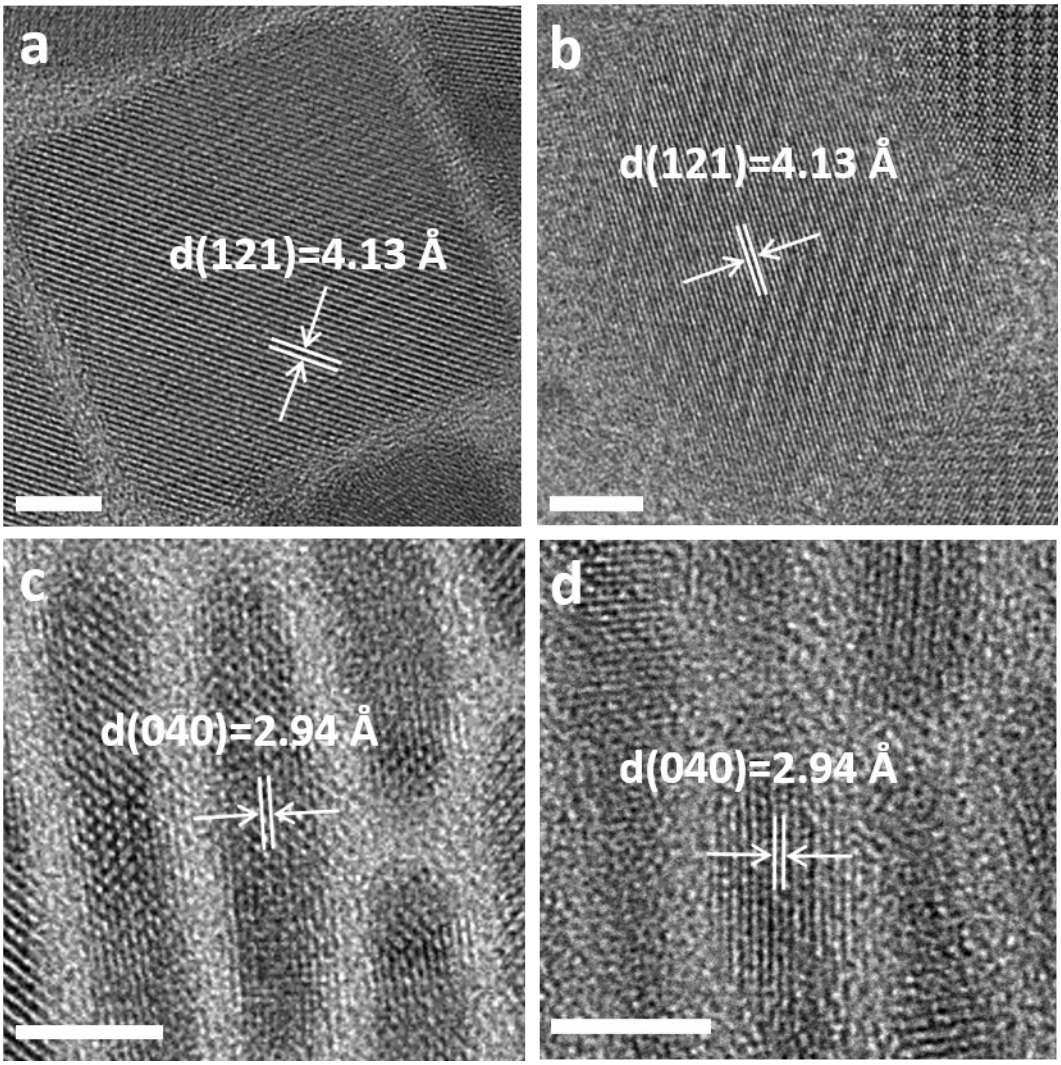

Fig. S14. *Top view (a-b) and side view (c-d) HRTEM images of the typical perovskite $CsPbBr_3$ NPLs collected from the top layer dispersion by centrifugation selection. The samples were synthesized in the open air, with Sn:Pb precursor ratios of 2:10 (a,c) and 5:10 (b,d), respectively. Each scale bar is 5 nm. The Sn precursor was $SnBr_2$.*

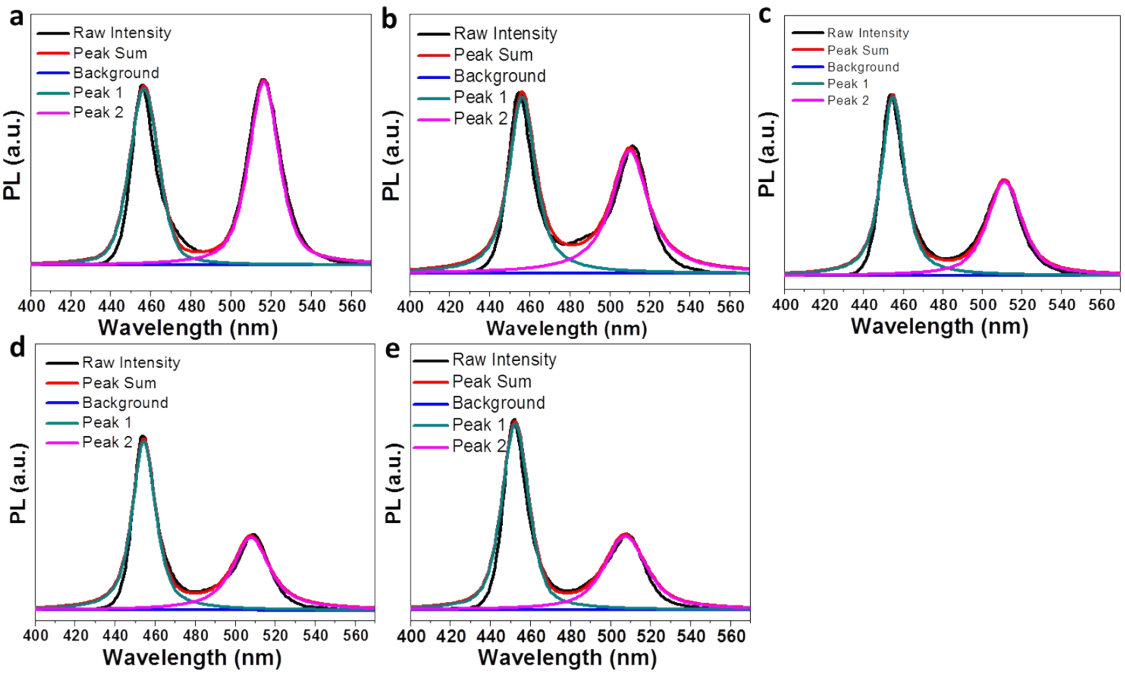

Fig. S15. *Multi-peak fitting of the PL spectra for the $CsPbBr_3$ nanocrystals achieved with precursor Sn:Pb ratios of 1:10 (a), 2:10 (b), 3:10 (c), 4:10 (d) and 5:10 (e). The multi-peak-emitting spectra were fitted by the type of Gaussian.*

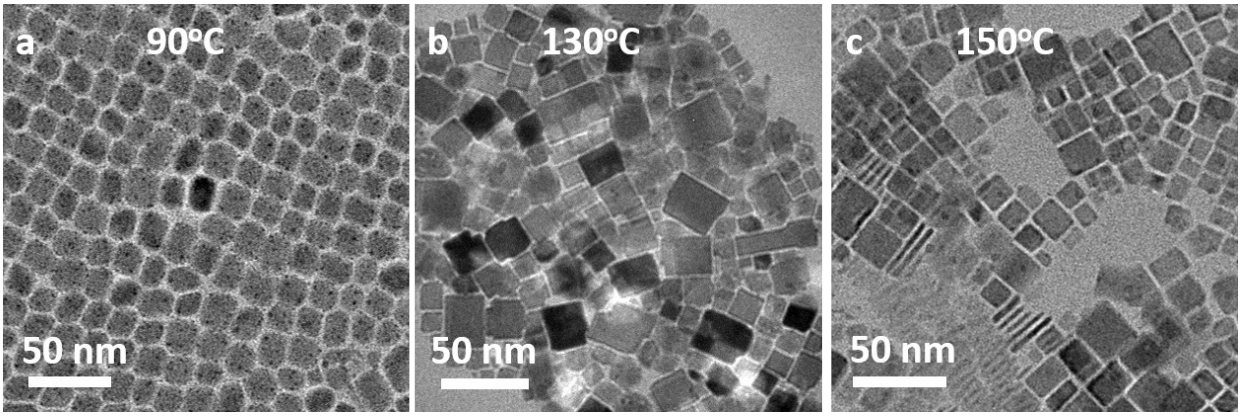

Fig. S16. *TEM images (a-c), optical absorbance spectra and PL (d) and XRD patterns (e) of the aliquots of the $CsPbBr_3$ nanocrystals achieved at different temperatures as dictated, in the presence of precursor Sn:Pb ratios of 2:10 in the open air.*

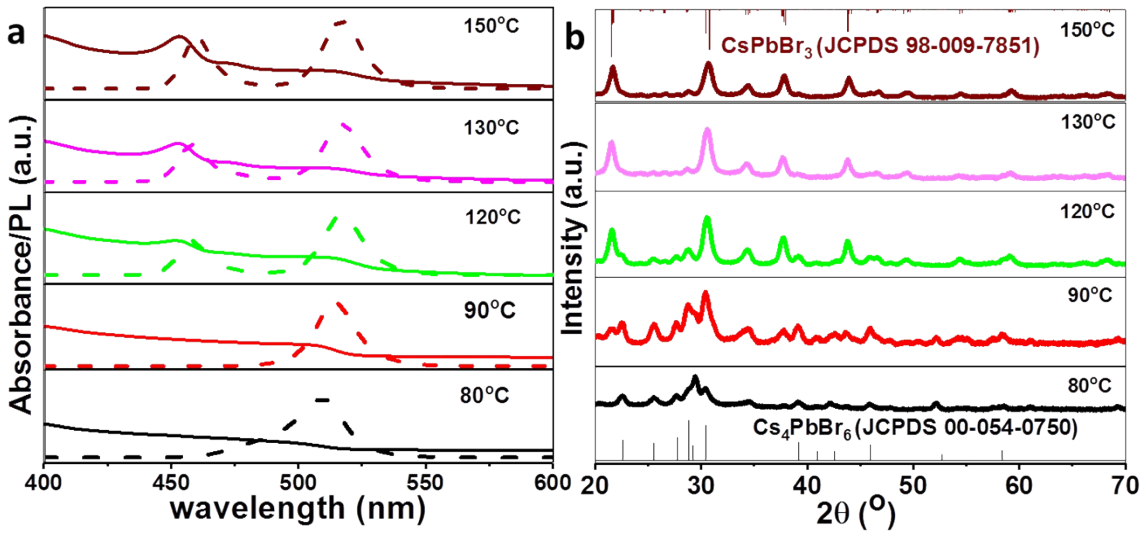

Fig. S17. *Optical absorbance spectra and PL (a) and XRD patterns (b) of the aliquots of the* $CsPbBr_3$ *nanocrystals achieved at different temperatures as dictated, in the presence of precursor Sn:Pb ratios of 2:10 in the open air.*

6. Characterization of the $CsPbCl_{3-x}Br_3$ nanocrystals synthesized in the presence of $SnCl_2$ in the open air

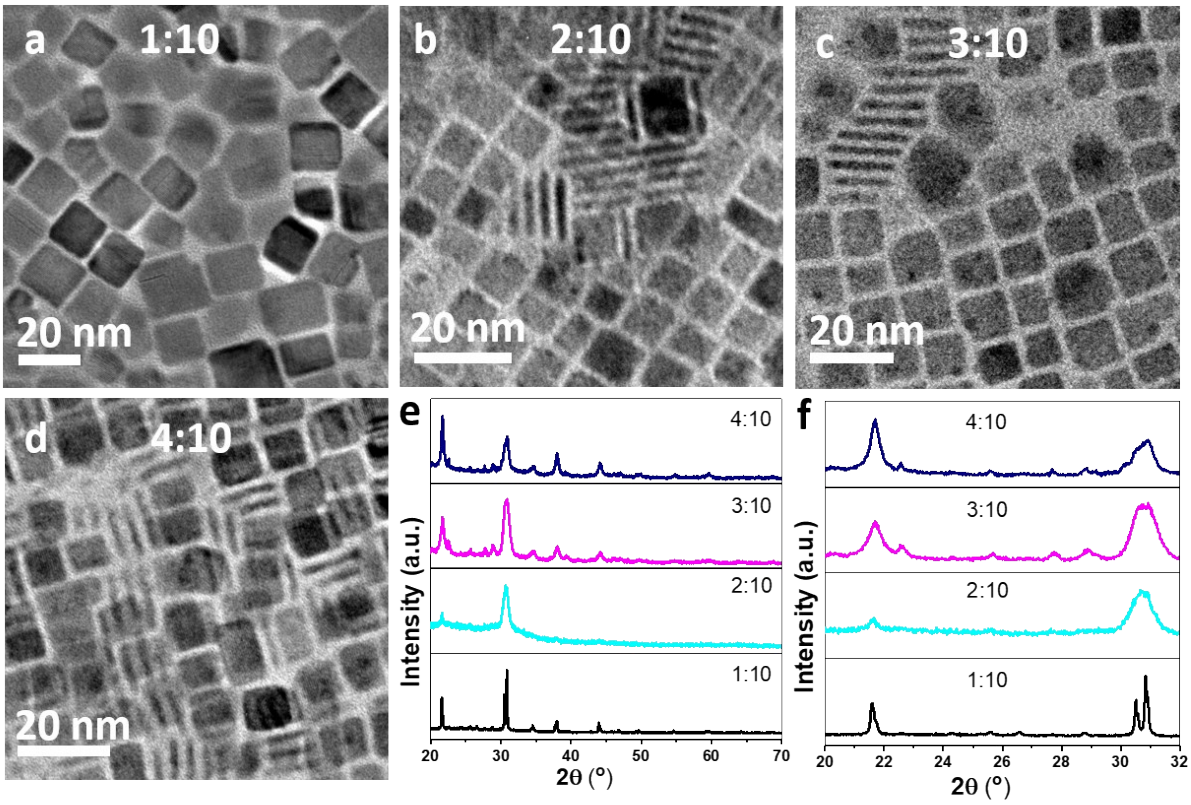

Fig. S18. *(a-d) TEM images and (e-f) XRD patterns of the perovskite $CsPbCl_{3-x}Br_3$ nanocrystals achieved in the presence of $SnCl_2$, in the open air, with precursor Sn:Pb ratios of 1:10 (a), 2:10 (b), 3:10 (c) and 4:10 (d), respectively. Panels b-e) display NPLs both standing edge-on perpendicular to the substrate and laying on the substrate.*

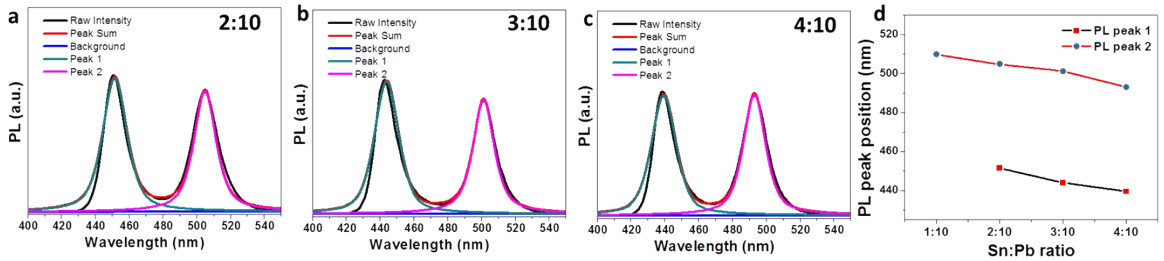

Fig. S19. *(a-c) Deconvolution of the PL spectra collected on the perovskite $CsPbCl_{3-x}Br_3$ nanocrystals of the $CsPbCl_{3-x}Br_3$ nanocrystals achieved in the presence of $SnCl_2$, in the open air, with different precursor Sn:Pb ratios as dictated. For data fitting, a doublet was used for each*

PL spectrum. (d) PL peak wavelength positions of the fitted peaks of the various $CsPbCl_{3-x}Br_3$ nanocrystals achieved with different precursor Sn:Pb ratios.

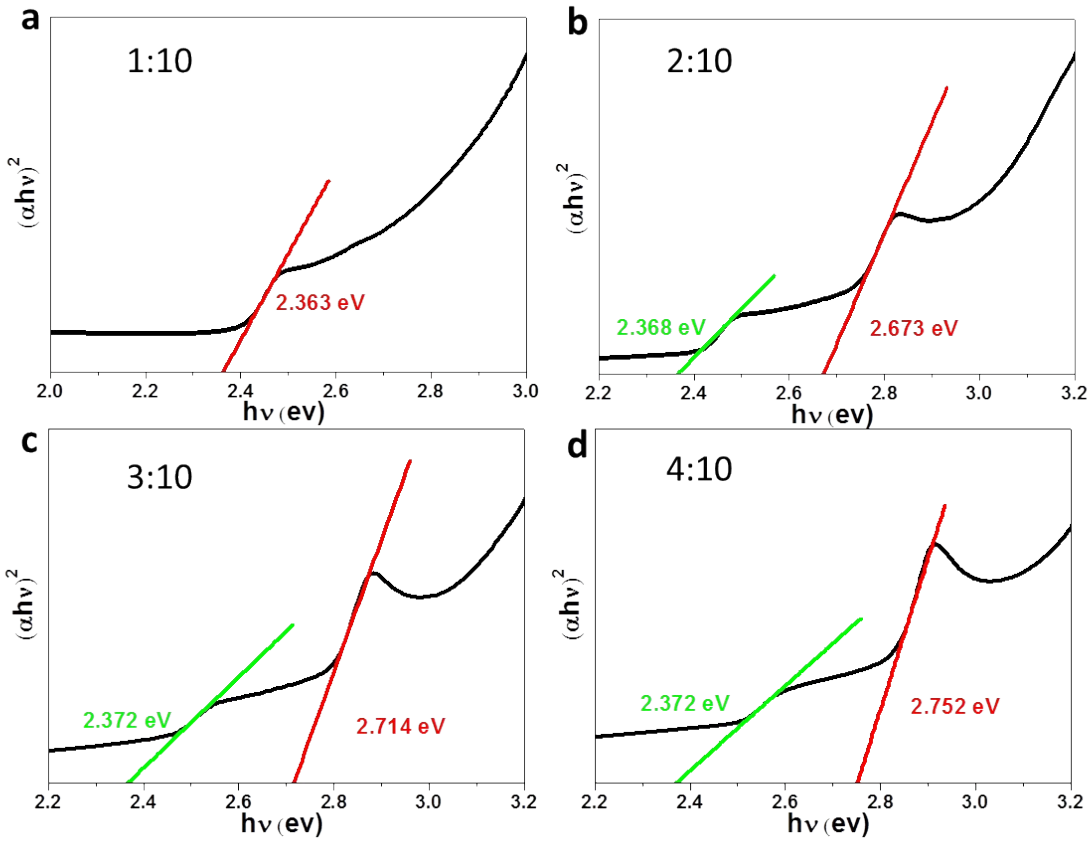

Fig. S20. *Tauc plots of various $CsPbCl_{3-x}Br_3$ nanocrystals formed in the presence of different precursor Sn:Pb ratios as dictated. The samples are prepared in the open air, in the presence of $SnBr_2$ in the open air.*

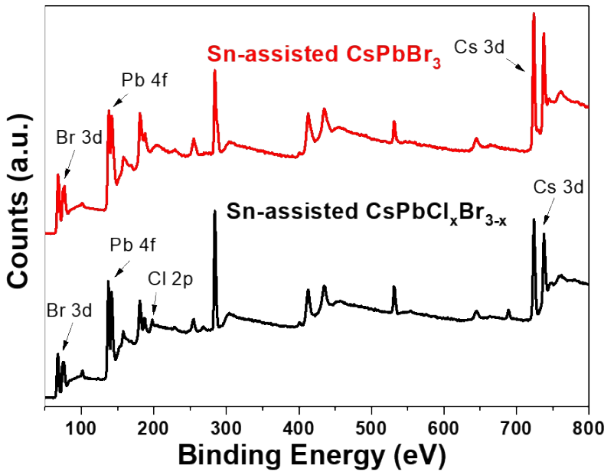

Fig. S21. *Survey XPS of the Sn-directed synthesized $CsPbBr_3$ nanocrystals and $CsPbCl_xBr_{3-x}$ in the open air, in the presence of $SnBr_2$ and $SnCl_2$, respectively. It is noteworthy that no Sn signal can be observed in all the as-synthesized samples. Cl signals is present in the sample collected when $SnCl_2$ is added.*

Table S2. *Photoluminesence quantum yields (PLQY) of the various $CsPbBr_3$ and $CsPbCl_xBr_{3-x}$ perovskite nanocrystals.*

Samples	PLQY (%)
$CsPbBr_3$ nanocrystals achieved in the absence of any Sn species	19.67
$CsPbBr_3$ nanocrystals achieved with precursor $SnBr_4$:$PbBr_2$ ratio of 2:10	29.30
$CsPbCl_xBr_{3-x}$ nanocrystals achieved with precursor $SnCl_4$:$PbBr_2$ ratio of 2:10	37.60
$CsPbBr_3$ nanocrystals achieved with precursor $SnBr_2$:$PbBr_2$ ratio of 3:10	80.20
$CsPbCl_xBr_{3-x}$ nanocrystals achieved with precursor $SnCl_2$:$PbBr_2$ ratio of 2:10	43.60

7. Characterization of the $CsPbBr_3$ nanocrystals synthesized in the presence of NaBr, tin acetate and $TiCl_4$, respectively

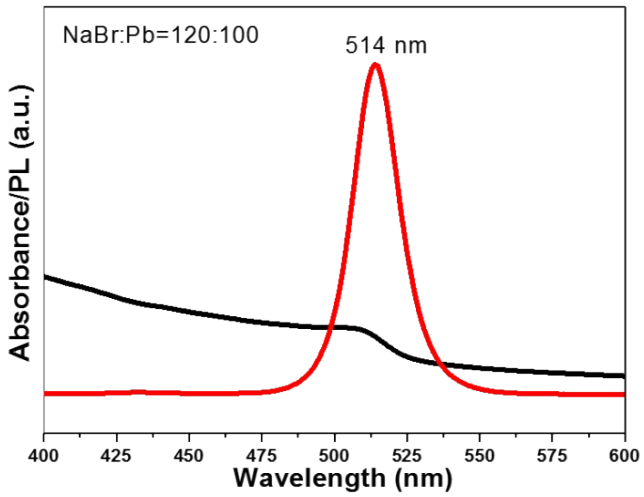

Fig. S22. *Optical absorbance spectra and PL the $CsPbBr_3$ nanocrystals achieved in the presence of excess NaBr by fixing the $NaBr:PbBr_2=120:100$.*

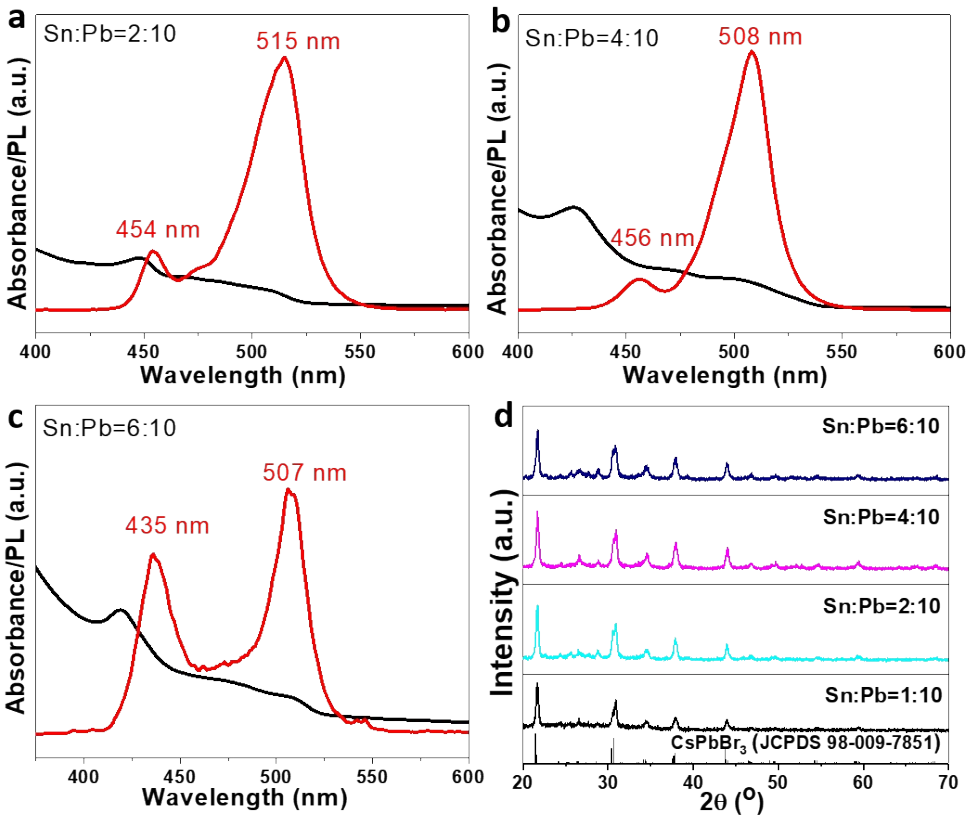

Fig. S23. *(a-c) Optical absorbance spectra and PL and (d) XRD patterns of the various $CsPbBr_3$ nanocrystals achieved with different amounts of $Sn(OAc)_2$ (labelled as Sn:Pb) as dictated, in the open air.*

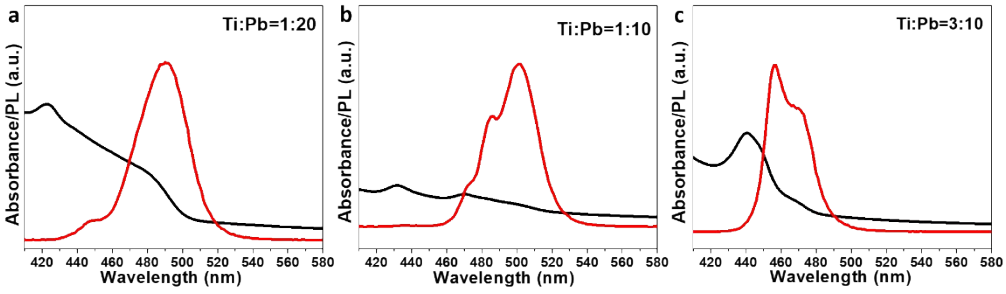

Fig. S24. *Optical absorbance spectra and PL of the $CsPbCl_xBr_{3-x}$ nanocrystals synthesized in the presence of different amounts of $TiCl_4$ (labelled as Ti:Pb ratio), at argon atmosphere.*

8. Characterization of the WLED devices

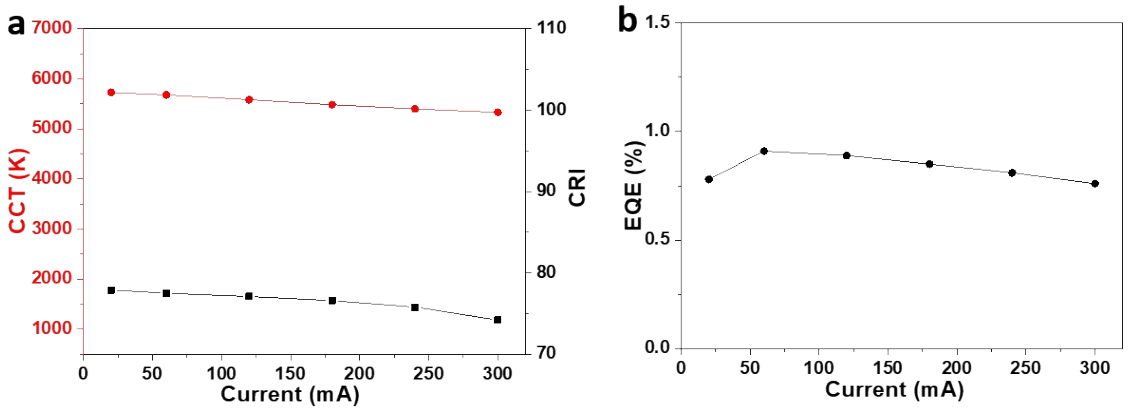

Fig. S25. *CCT and CRI (a), and EQE (b) values of the $CsPbBr_3$-based WLED lamp under different drive currents*

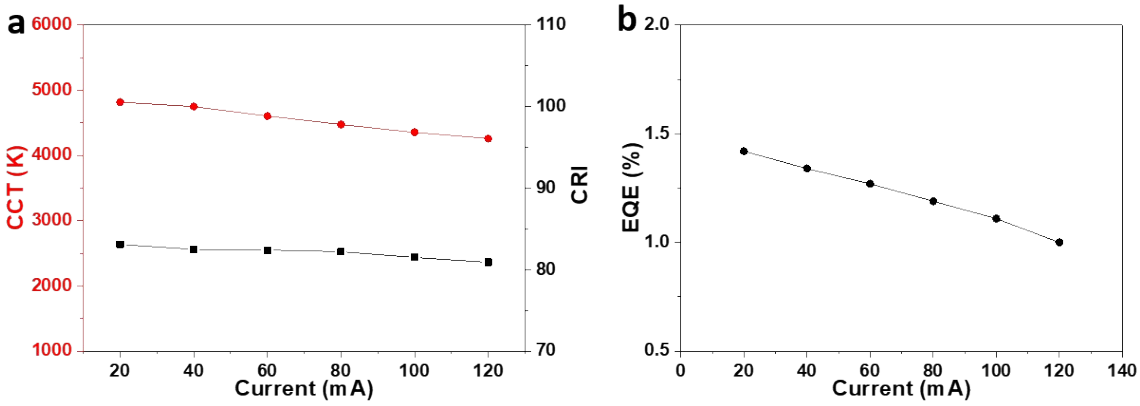

Fig. S26. *CCT and CRI (a), and EQE (b) values of the Sn-$CsPbBr_3$-based WLED lamp under different drive currents.*

Table S3. *CIE color coordinates (x, y), CRI, CCT, EQE and luminous efficacy of $CsPbBr_3$-based WLED.*

WLED	I(mA)	CIE(x)	CIE(y)	CRI	CCT (K)	EQE	Luminous efficacy (lm/W)
1	20	0.3269	0.3554	77.9	5730	0.78%	1.53
2	60	0.3283	0.3481	77.5	5680	0.91%	1.68
3	120	0.3305	0.3434	77.1	5585	0.89%	1.57
4	180	0.3328	0.338	76.6	5484	0.85%	1.41
5	240	0.3345	0.3322	75.8	5401	0.81%	1.28
6	300	0.3357	0.3255	74.2	5332	0.76%	1.16

Table S4. *CIE color coordinates (x, y), CRI, CCT, EQE and luminous efficacy of Sn-$CsPbBr_3$-based WLED.*

WLED	I(mA)	CIE(x)	CIE(y)	CRI	CCT(K)	EQE	Luminous efficacy (lm/W)
1	20	0.3513	0.3634	83.1	4820	1.42%	2.83
2	40	0.3516	0.3512	82.7	4752	1.34%	2.72
3	60	0.3547	0.3455	82.4	4607	1.27%	2.27
4	80	0.3574	0.3412	82.2	4478	1.19%	2.06
5	100	0.3597	0.3366	81.5	4356	1.11%	1.83
6	120	0.3615	0.3328	80.9	4261	1.00%	1.62

9. Anions exchange on the as-synthesized $CsPbBr_3$ nanocrystals

Preparation of $PbCl_2$ and PbI_2 stock solution. PbX_2 (X=Cl, I) stock solutions were prepared by using modified procedures previously-reported by Manna and co-workers. In the case of $PbCl_2$ solution, $PbCl_2$ (83.3 mg, 0.3 mmol), TOP (1.0 ml), OA (0.5 mL), OM (0.5 ml), and ODE (7.5 ml) were loaded into a 50 mL three-neck flask. The temperature was then raised to 140 ^oC under vacuum and kept at 140 ^oC for 60 min. The resulting $PbBr_2$ stock solution was cooled to RT, transferred to a vial and stored in the glove box for further use. For PbI_2 solution, PbI_2 (138 mg, 0.4 mmol), OA (0.375 ml), OM (0.375 ml), and ODE (7.5 ml) were loaded into a 50 ml three-neck flask, followed by raising the temperature to 130 ^oC under vacuum and keeping it for 60 min. The resulting PbI_2 stock solution was cooled to RT for further use.

Anion exchange reactions. Anion exchange was performed in the Ar-filled glovebox, by using a modified procedure described by Akkerman *et al*.[1] Typically, different quantities (normally ranging from 10 to 500 μL) of 0.06 M halide precursors solution were swiftly injected in 10 vials, each holding 3 mL of diluted crude $CsPbBr_3$ NC solution (in haxane). The reactions were kept for 1 h and the dispersions were transferred in the cuvettes for subsequent optical tests.

Both the UV-Vis absorption and PL emission spectra of the $CsPbCl_xBr_{3-x}$ nanocrystals collected by ion exchange with Cl^- showed a blue shift with increasing the $PbCl_2$ fraction in the exchange reaction (Fig. S36). However, the UV-Vis-NIR absorption and PL emission spectra of the $CsPbI_xBr_{3-x}$ nanocrystals collected by ion exchange with I^- are red-shifted after the introduction of I^- ions (Fig. S37). We noticed that the nanocrystals are not stable and the increasing amount of I^- or Cl^- ions led to the damping intensity of the shorter wavelength emission.

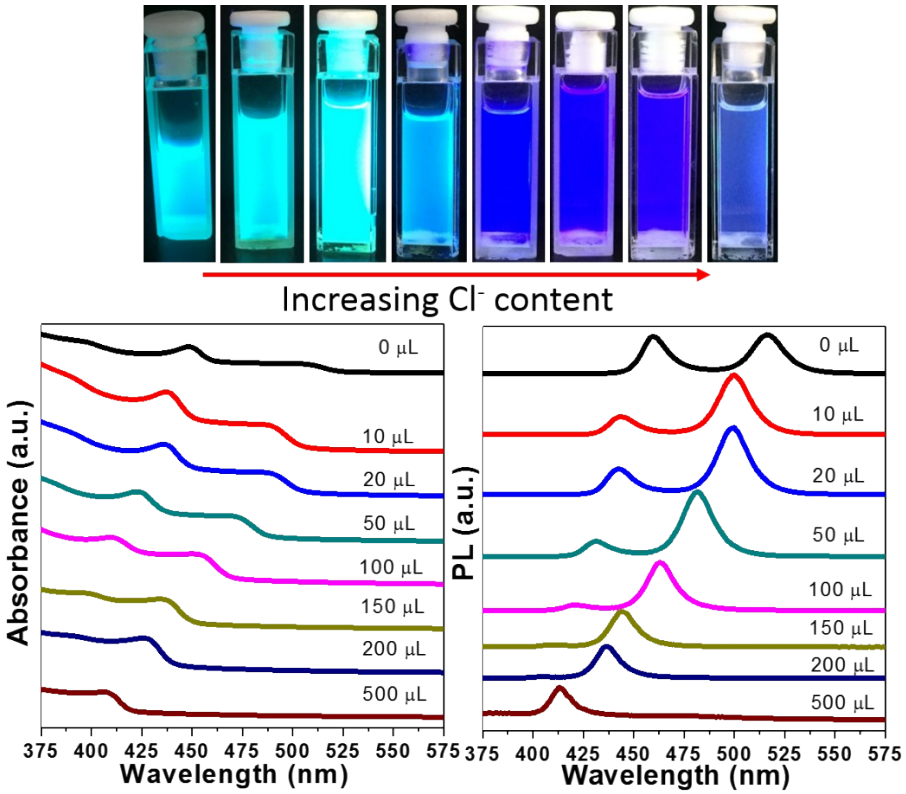

Fig. S27. *(a) Optical absorbance spectra and (b) PL spectra of the various* $CsPbCl_xBr_{3-x}$ *nanocrystals achieved by anion exchange of the as-synthesized CsPbBr3 in the presence of different amounts of* Cl^- *ions as dictated. The top panel presents the photographs of corresponding nanocrystals dispersed in hexane under UV light illumination (355 nm excitation wavelength).*

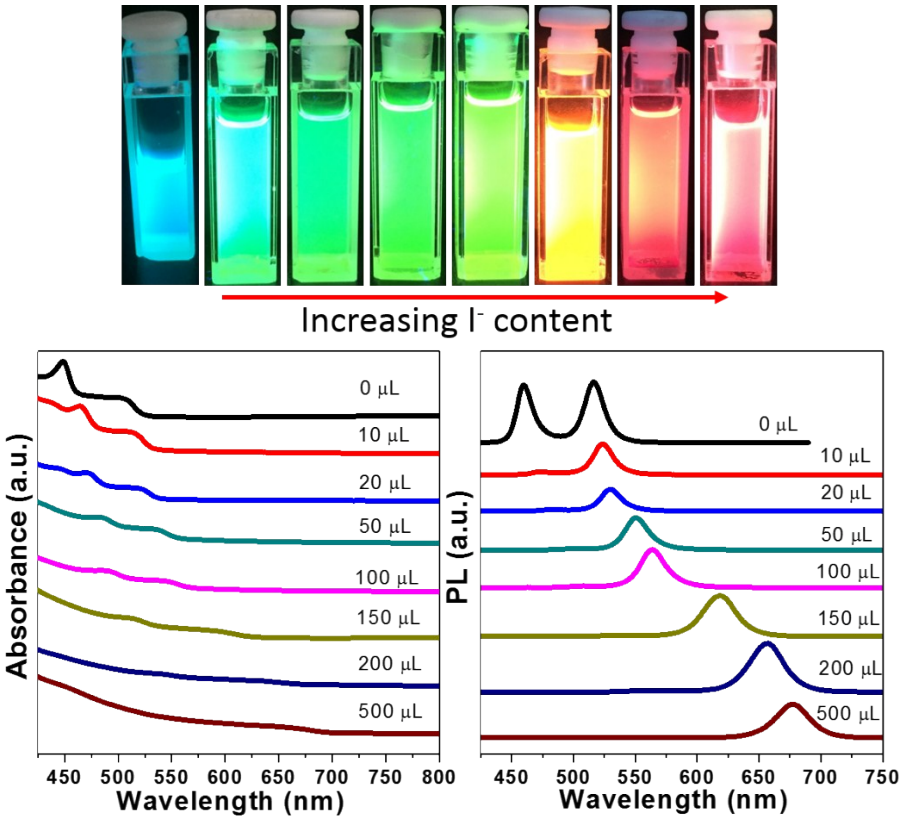

Fig. S28. *(a) Optical absorbance spectra and (b) PL spectra of the various* $CsPbI_xBr_{3-x}$ *nanocrystals achieved by anion exchange of the as-synthesized CsPbBr3 in the presence of different amounts of* I^- *ions as dictated. The top panel presents the photographs of corresponding nanocrystals dispersed in hexane under UV light illumination (355 nm excitation wavelength).*

References

[1] Q.A. Akkerman, V. D'Innocenzo, S. Accornero, A. Scarpellini, A. Petrozza, M. Prato, L. Manna, Tuning the Optical Properties of Cesium Lead Halide Perovskite Nanocrystals by Anion Exchange Reactions, J. Am. Chem. Soc. 137 (2015) 10276-10281.